Electronic Supplementary Material (ESI) for Nanoscale.
This journal is © The Royal Society of Chemistry 2017

Supplementary information

One-dimension Random Laser based on Artificial High-index Contrast Scatters

Yanyan Wu,[1] Yuhao Ren,[1] Anqi Chen,[1] Zhiyang Chen,[1] Yunfeng Liang,[1] Jinyu Li,[1] Guanlin Lou,[1] Hai Zhu,[1*] Xuchun Gui,[2] Shuangpeng Wang[3] and Zikang Tang[3*]

[1]State Key Laboratory of Optoelectronic Materials and Technologies, School of Physics, Sun Yat-Sen University, Guangzhou 510275, China

[2]State Key Laboratory of Optoelectronic Materials and Technologies, School of Electronics and Information Technology, Sun Yat-Sen University, Guangzhou 510275, China

[3]The Institute of Applied Physics and Materials Engineering, University of Macau, Avenida da Universidade, Taipa, Macau

E-mail: zhuhai5@mail.sysu.edu.cn (Hai Zhu), zktang@umac.mo (Zikang Tang)

I. Material synthesis and optical properties

The ZnO MWs were synthesized by using the typical vapor-liquid-solid technique. The quartz boat coated with gold was acted as catalyst, and the Zn source powder-thermal was evaporated in the air. The growth temperature was controlled in the range from 950 to 980 ℃. The air transported the evaporated Zn and suppled oxygen. Based on this method, the largest length of the grown ZnO microwires can approach 10 mm with the diameters of 20-30 μm (Figure S1a). Subsequently, the as-growth MWs were picked from the quartz boat and then transferred to the sapphire substrate. Atom-force microscopy (AFM) experiment had been done to investigate the morphology about border of MW.

The AFM image in Figure S1a (bottom part) shows smooth morphology of the as-grown MW with roughness below 12 nm. The XRD spectrum of MW array indicates that the ZnO MW was hexagonal crystal structure with c-axis preferred orientation (Figure S1c). To explore the detail feature of the optical characteristic of MW, the room-temperature PL measurement was performed (Figure S1b). The typical near bandedge emission (NBE) peak dominates in the spectra at 300 K with quite low defect peak.

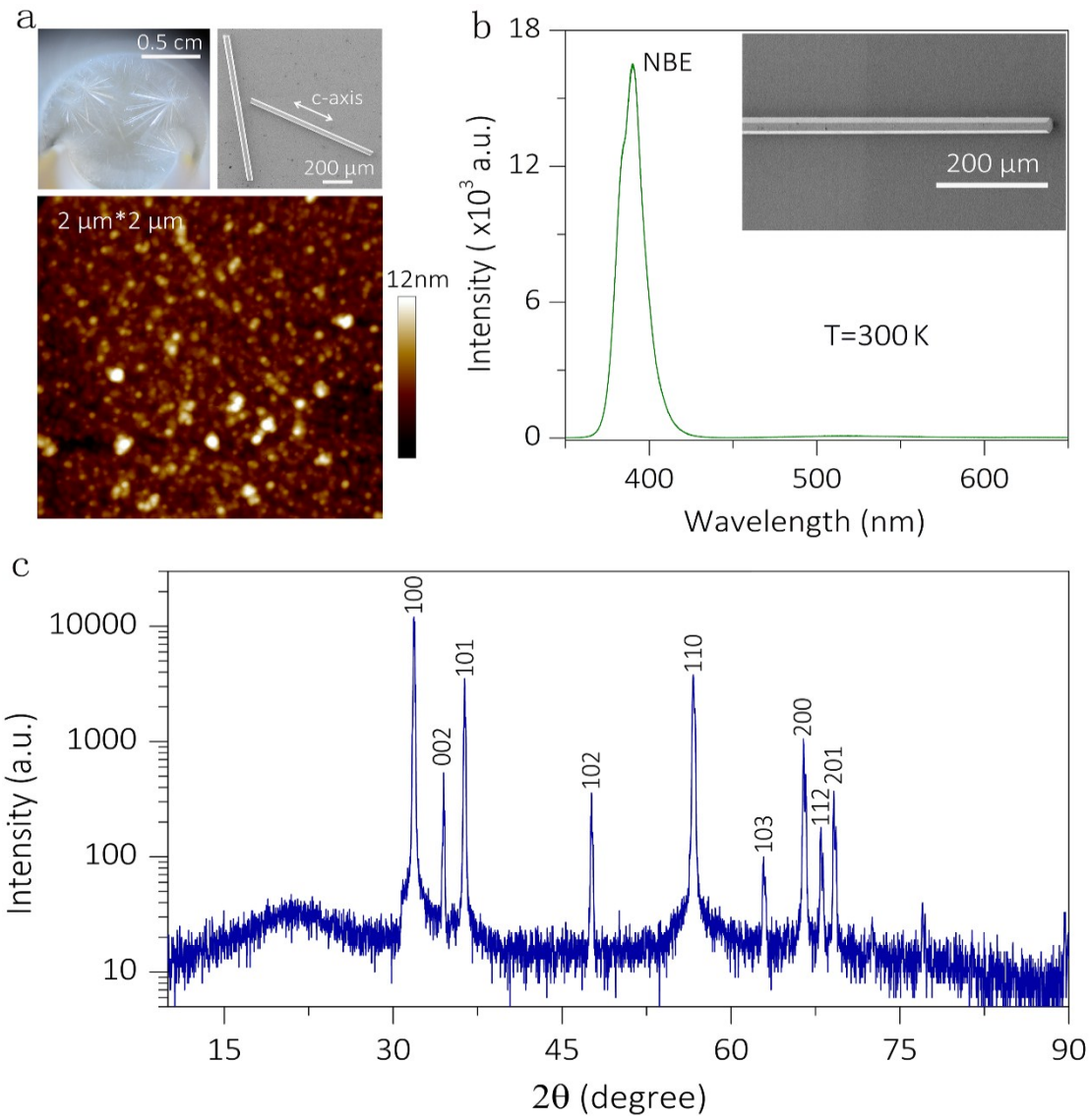

Figure S1. The crystalline and optical properties of ZnO MWs. (a) Top: Photon image of ZnO MWs grown in the quartz tube, and the top-view SEM image of the MW. Bottom: The AFM image about one border of MW. (b) The PL spectra of single ZnO MW at room temperature (300 K). Inset: Top-view

enlarged SEM image of MW at one end. (c) XRD spectrum of ZnO MW array.

II. Sample fabrication

We fabricated a series of ZnO MWs with different densities of micro-pits with the same profile intentionally. The Q-switch Nd:YAG (266 nm) nanosecond pulsed laser (50 Hz repetition rate, 30 ns pulse width) beam was focused into a spot of several micron in diameter through an objective (13×). The focused beam was vertically incident on the side surface of ZnO MW for a few second and then an air micro-pit was fabricated on the side surface. Moreover, the average spacing of the micro-pits chain can be controlled using the delay stage.

III. Lasing characteristic measurements

The lasing characteristic of the 1D MW random laser were measured by our home-build micro-photoluminescence set-up. For the measurement, the pulsed Nd:YAG (266 nm) nanosecond laser (30 Hz repetition rate and 30 ns pulse duration) was used as the pumping source. The pumping laser was focused on the sample by a cylindrical lens. The laser beam was focused into a strip of 5 mm (length) and 50 μm (width) along the c-axis of MW. The emission signal was collected from one end face of side edge using an objective (13×), and recorded by a spectrometer (SP-750i, Princeton Instruments).

For the angular resolved PL measurements, the emission from end facet was collected and collimated by an objective (13×, NA=0.2). The collimated light was detected by a single mode optical fiber and recorded by a spectrometer (2000PRO Ocean Optical). Here, the optical fiber was mounted on a delay stage with resolution of 1.0 μm, and moved perpendicular to the c-axis of MW.

For investigating the spatial profile of radiation, the pumping and collecting configuration were identical to the PL measurement, and the pattern was recorded by a laser beam profile analysis (Spiricon Ophir Photonics). All the measurements were performed at room temperature.

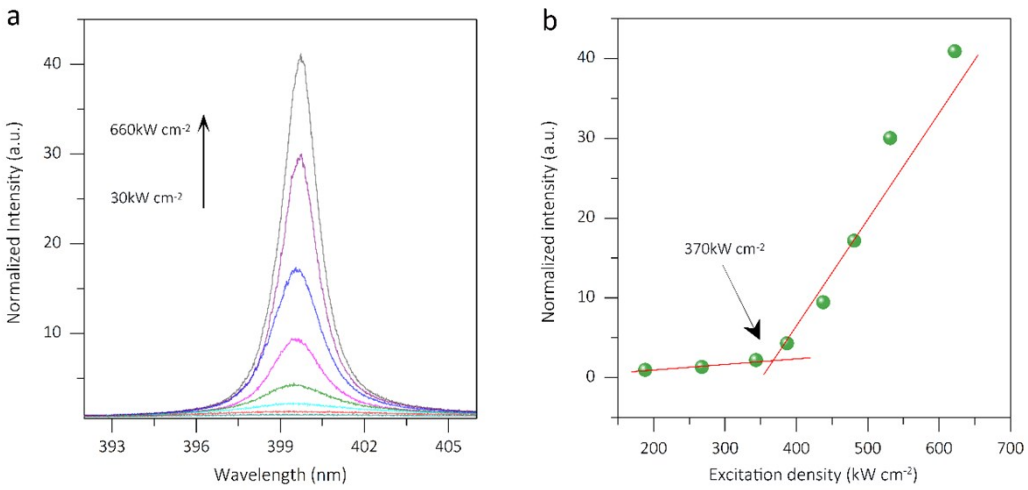

Figure S2. (a) Emission spectra of sample B as a function of pumping intensity. (b) The illustration of output intensity versus the pumping power for sample B.

The emission spectra of the as-grown sample B with different excitation intensity were shown Figure. S2a. A broad spontaneous emission band centered at 399 nm can be seen in the spectrum under low pumping power (< 370 kW cm^{-2}). The ASE threshold of Sample B was extracted to be about 370 kW cm^{-2} from the L-L curve (Figure. S2b).

Figure. S3a presents the schematic diagram and SEM images of fabricated sample C with the random micro-pits. The spacing of adjacent micro-pits was varied from 50 μm to 70 μm. As shown in Figure. S3b, strong scatter light can also be seen from the micro-pits position beside the end facets, which indicates that the micro-pits have strong scattering effect on the light transmission. In addition, the distribution of radiation on the end facet is uniform for the sample C rather than concentrating on the hexagonal boundary of the MW (Figure. S3c), which results from scattering of the micro-pits in the MW. The spatial profile of sample C RL (far-field radiation) exhibits a quasi-Gaussian type distribution, as shown in Figure. S3d.

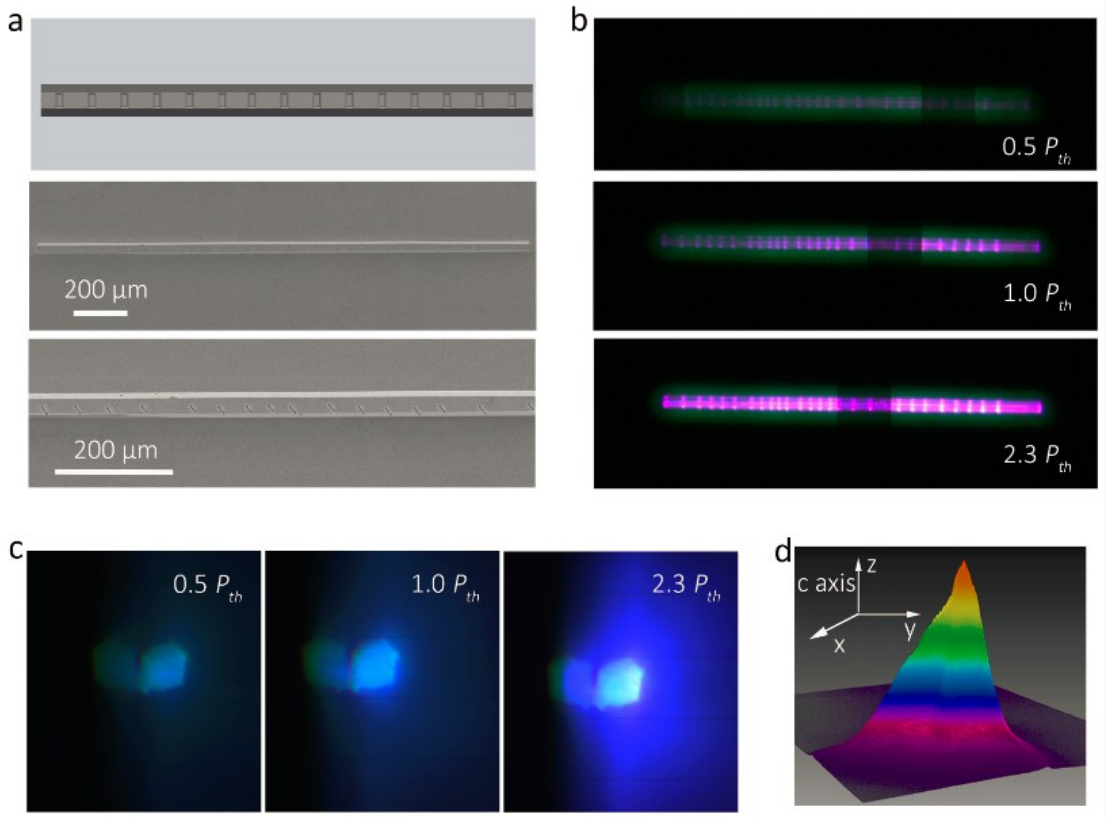

Figure S3. (a) The schematic diagram and SEM images of sample C with high density micro-pits in the MW. (b) The top-view emission images of sample C with different pumping power. (c) The near-field radiation patterns of sample C under different excitation power. With the increasing of the power, the uniform emission from end facet was transited from the spontaneous emission to the stimulated emission. Noticeable, the nearby weak emission spot was originated from the mirror image of substrate. (d) Measured far-field intensity profile of the 1D MW RL.

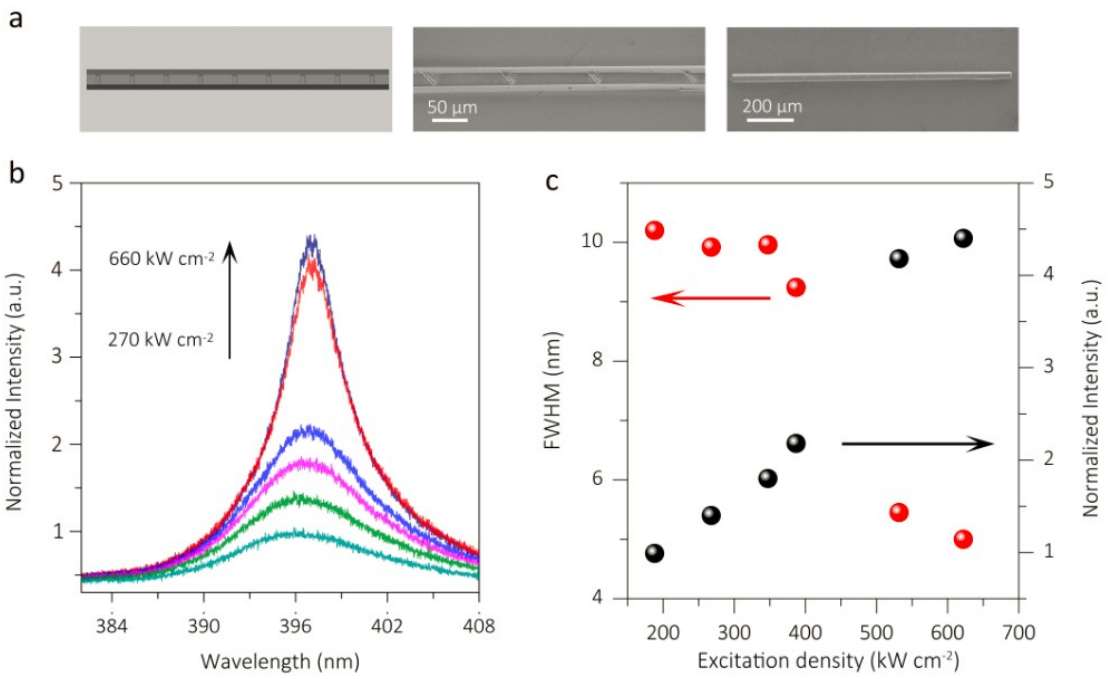

Figure S4. Optical features of the ZnO MW with low-density micro-pits. (a) The schematic diagram and top-view SEM images of MW with the average spacing of about 100 μm. (b) The typical ASE spectra under different pumping density. (c) The integrated emission intensity and FWHM of peak versus the excitation intensity, respectively.

In order to furtherly study the relation between spacing and characters of random lasing, ZnO MW with low-density micro-pits (Figure. S4a) and with high-density micro-pits (Figure. S5a) had been fabricated, meanwhile their optical properties were investigated, respectively. The ASE peak dominants in the spectra of the MW with low-density micro-pits under high excitation power (Figure. S4). While, only a single broad spontaneous emission band can be observed in the spectra for the MW with high-density micro-pits even when the pumping power exceeds the 660 kW cm^{-2} (Figure. S5b). The intensity of emission peak has a linear relationship with the excitation intensity, and the peak exhibits no narrow behavior with the increasing of excitation power (Figure. S5c).

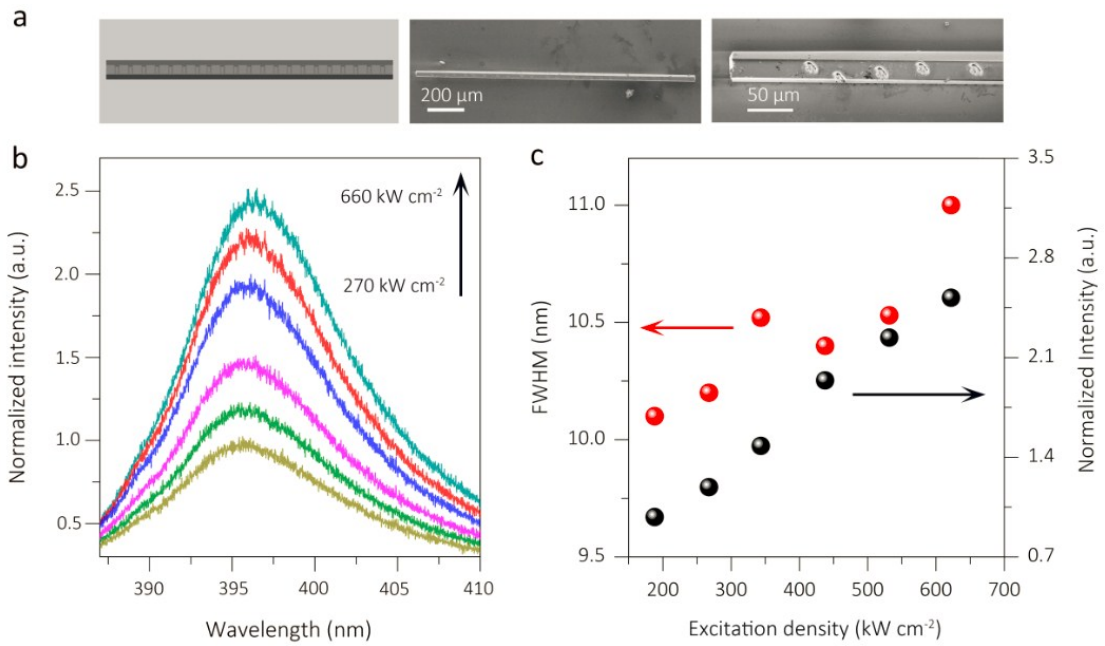

Figure S5. Optical features of the ZnO MW with high-density micro-pits. (a) The schematic diagram and SEM images of the single MW with the average spacing of about 40 μm. (b) Emission spectra under different pumping intensity. (c) Integrated emission intensity and FWHM of peak versus the excitation intensity, respectively.